FEBS Letters 589 (2015) 555–564

journal homepage: www.FEBSLetters.org

c-MYB regulates cell growth and DNA damage repair through modulating MiR-143

Wenjun Wang [a,1], Sipei Wu [b,1], Yongsheng Shi [c], Yong Miao [c], Xiaojun Luo [c], Mei Ji [d], Kaitai Yao [e], Jianxing He [a,*]

[a] State Key Laboratory of Respiratory Diseases, Guangzhou Institute of Respiratory Disease, The First Affiliated Hospital of Guangzhou Medical University, Guangzhou 510120, China
[b] Lung Cancer Research Institute and Cancer Center, Guangdong Provincial People's Hospital, Guangzhou 510080, China
[c] Nanfang Hospital, Southern Medical University, Guangzhou, Guangdong 510515, China
[d] Department of Gynecology, The First Affiliated Hospital of Zhengzhou University, Zhengzhou 250117, China
[e] Cancer Institute, Southern Medical University, Guangzhou, Guangdong 510515, China

ARTICLE INFO

Article history:
Received 24 October 2014
Revised 23 December 2014
Accepted 13 January 2015
Available online 20 January 2015

Edited by Lukas Huber

Keywords:
c-MYB
miR-143
Cancer stem cell
Radio-resistivity
Nasopharyngeal carcinoma

ABSTRACT

Radiotherapy is the most successful nonsurgical treatment for nasopharyngeal carcinoma (NCP). Although NPCs initially respond well to a full course of radiation, recurrence and metastasis are frequent. In this study, we found that down-regulated c-MYB expression was associated with increased radiation resistance and DNA damage repair ability. Interestingly, c-MYB was over-expressed in cancer tissues but not in the adjacent tissues. Down-regulation of c-MYB expression inhibited cell proliferation, and led to cell cycle arrest at the M phase in NPC cells. Luciferase and chromatin immunoprecipitation assays demonstrated that c-MYB transactivated miR-143 through direct binding to its promoter. Based on these results, c-MYB might target miR-143 in order to regulate stem cell properties, cell growth, apoptosis, and DNA damage repair.

1. Introduction

The c-MYB protein is a transcription factor [1] that plays a key role in the cell cycle regulation, proliferation, and differentiation of hematopoietic cells. High expression levels of c-MYB were first found in immature bone marrow hematopoietic cells and thymocytes, and subsequently in the neuroectodermal gastrointestinal epithelium and vascular smooth muscle cells. Recent studies have also shown that abnormal expression of c-MYB can lead to colon, breast, and gastro-esophageal cancer [2]. c-MYB can activate crucial target genes related to cancer progression and metastasis, including Sox-2, Bcl-2, Bax, and c-MYC [3]. Studies have indicated that the transcription factor MYB governs intestinal stem cell gene expression through the Wnt signaling pathway and thereby affects tumor cell self-renewal [4]. MicroRNAs (miRNAs) are an extensive class of 18–24-nucleotide long non-coding RNAs that regulate gene expression at the post-transcriptional level [5]. They have been reported to play an important role in the development, proliferation, and differentiation of various types of cells [6–8]. MiRNAs have also been linked to radio- and chemoresistance [9]. Recent studies have indicated that the expression of miRNA-143 was significantly down-regulated in several human neoplasms including colon, ovarian, esophageal, and bladder cancer [10,11]. Noguchi et al. reported that miR-143 inhibits cell growth through down-regulation of the translational expression level of ERK5 and AKT [12]. In addition, Lin et al. showed that miR-143 targeted the *RAS* oncogene, contributing to inhibition of tumor invasion and metastasis [13]. Radiation therapy is the main treatment for nasopharyngeal carcinoma (NPC). However, patients with an early diagnosis who receive radiation therapy nonetheless experience frequent recurrence. During the past in the last decades, evidence has been provided that the cancer stem cell (CSC) content and intrinsic radiosensitivity can affect their radiocurability potential. In this study, we detected the level of expression of c-MYB and miR-143 in normal nasopharyngeal and NPC tissues. Furthermore, we analyzed the relationships between the expression levels of c-MYB and the clinicopathological parameters of NPC patients. We also studied the effects of c-MYB on cell growth and its radiation-resistant mechanism in NPC cells, with the aim of determining a novel potential therapeutic approach for the treatment of NPC.

* Corresponding author.
E-mail address: hejx@vip.163.com (J. He).
[1] These authors contributed equally to this work.

http://dx.doi.org/10.1016/j.febslet.2015.01.012
0014-5793/

2. Materials and methods

2.1. Cell culture

Human NPC cell lines, c666-1, 5-8F, CNE1 and CNE2, were maintained in RPMI 1640 culture (Life Technologies, Carlsbad, CA) supplemented with 10% fetal bovine serum (FBS), 100 units/mL penicillin G and 100 μg/mL streptomycin. Np69 cells were maintained in Keratinocyte-SFM culture (GIBCO, USA). All the cells were maintained in a humidified 5% CO_2 incubator at 37 °C, all the cell lines we used without EBV infection.

2.2. Tumorsphere formation assay

Tumorsphere culture was performed as described previously [20]. For sphere formation assay, 500–800 single cells/well are seeded in serum-free DMEM-F12 supplemented with 1 × B27 (Life Technologies), 20 ng/mL epidermal growth factor, and 20 ng/mL basic fibroblast growth factor in ultralow attachment (ULA) plate. Medium was replenished every 4 days and spheres counted within 2 weeks. For secondary (2°) sphere formation assay, the 1° spheres were trypsinized into single cells and reseeded (500 cells/well) in the ULA plate. The 2° spheres were counted in ~10 days. The 2° spheres >50 μm were counted by microscope.

2.3. Radiation assay

The NPC cells after c-MYB inhibitor or co-treatment with c-MYB inhibitor and miR-143 were irradiated with 8 Gy of 160 kV X-rays using RS 2000 X-ray Biological Irradiator (Rad Source Technologies, USA) at a dose rate of 1 Gy/min. and co-treated w cells to X-ray to determine their radiation sensitivity differences. Cells were collected for Western blot, cell cycle and apoptosis assay after irradiated 12 h. Experiments were run in triplicate.

2.4. Aldefluor assay

The Aldefluor assay was carried out according to manufacturer's guidelines. Briefly, 1×10^6 single cells obtained from cell cultures were suspended in 1 ml Aldefluor assay buffer containing an ALDH substrate, 5 μL Aldefluor reagent, and were incubated for 45 min at 37 °C with continuous mixing. Subsequently, flow cytometry was used to measure the ALDH-positive cell population.

2.5. Quantitative real-time PCR

Total RNA was extracted using the TRIzol® reagent (Invitrogen, Carlsbad, CA, USA) and the resulting mRNA was reverse transcribed into cDNA using 5× PrimeScript RT Master Mix (TaKaRa Bio Group, Dalian, China). The reaction conducted at 37 °C for 15 min and 85 °C for 5 s, according to the manufacturer's protocol. Quantitative PCR (qPCR) was performed using 2× SYBR Premix Ex Taq (TaKaRa Bio Group, Dalian, China) with a 7300 ABI real-time PCR System (Applied Biosystems, Foster City, CA, USA) under the following conditions: 95 °C for 30 s, 95 °C for 5 s and 60 °C for 31 s for 40 cycles. The relative mRNA levels were analyzed by the $2(^{-\triangle\triangle}Ct)$ method with GAPDH as an internal control. Primers used for real-time PCR were: c-MYB forward, 5′-GCCAATTATCTCCCGAATCGA-3′ and c-MYB reverse, 5′-ACCAACGTTTCGGACCGTA-3′ (Table S1).

The details of patients and tissue samples, immunohistochemistry (IHC), antibodies, Western blotting and immunofluorescence, clonogenic survival assays, cell proliferation, quantitative luciferase assay, cell cycle and apoptosis assay are in Doc S1.

2.6. Statistical analysis

All experiments were repeated at least three times. The data was expressed as the mean value ± standard deviation (S.D.). The findings were considered significant at a P value of <0.05. All statistical analyses were performed by the v5.0 GraphPad Prism Program, (GraphPad Software Inc., SanDiego, CA, USA).

3. Results

3.1. The expression of MiR-143 and c-MYB in human tumor cell lines and clinical specimens

c-MYB was previously found to regulate the cell cycle, proliferation, and differentiation of hematopoietic cells [1]. To verify the role of c-MYB in NPC in vivo, a panel of human tumor cell lines was first analyzed to quantitate the expression level of c-MYB. In order to link miR-143 with NPC, we performed q-RT-PCR in 4 NPC cell lines and found that the miR-143 expression levels were lower in NPC undifferentiated C666-1, low-differentiated CNE-2, and 5-8F cell lines compared to the highly differentiated CNE-1 and immortalized non-tumorigenic NP69 cell lines, which' were negatively correlated with c-MYB expression (Fig. 1A and B). We further examined the expression levels of miR-143 and c-MYB in specimens obtained from 105 cases of nasopharyngeal carcinoma and adjacent tissues, 31 cases of normal nasopharyngeal epithelial. Consistent with the data obtained from tumor cell lines, the average expression level of miR-143 was significantly lower in malignant tumor cells, whereas c-MYB expression was increased in these cells compared to non-tumorigenic NP69 cells (Fig. 1C and D).

3.2. Immunohistochemical analysis of c-MYB and miR-143 expression in NPC tissues

We measured the expression levels and subcellular localization of c-MYB and miR-143 protein in 105 archived paraffin-embedded NPC samples using immunohistochemical staining. The relationship between clinicopathological characteristics and c-MYB and miR-143 expression levels in individuals with NPC are summarized in Table 1. c-MYB and miR-143 expression in the nucleus was significantly related to the T classification (T1–T2 vs. T3–T4; $P = 0.027$ and $P = 0.009$, respectively), N classification (N0–N1 vs. N2–N3; $P = 0.020$ and $P = 0.01$, respectively), distant metastasis ($P = 0.000$ and $P = 0.007$, respectively), and clinical stage (I–II vs. III–IV; $P = 0.000$ and $P = 0.000$, respectively), whereas it was not associated with the patients' gender, age, or histological subtype ($P > 0.05$). These results indicated that tumor invasion beyond the muscularis propria, positive lymph node metastasis, positive lymphatic invasion, and progressive stage were all associated with abnormal expression of c-MYB. In primary tumors, high expression of c-MYB was significantly associated with decreased miR-143 expression (Fig. 2A, Spearman correlation coefficient, 0.2851; $P = 0.000$).

To further demonstrate the value of c-MYB expression in predicting survival of NPC patients, as shown in Fig. 2B and C, Kaplan–Meier curves and log-rank survival tests suggested that miR-143 and c-MYB expression in NPC patients was associated with survival time, with significantly increased overall survival of patients with high miR-143 expression in their NPC lesions compared to those with low miR-143 expression ($P < 0.0001$). In contrast, the overall survival of patients with high expression of c-MYB in their NPC lesions was significantly reduced compared to those with low c-MYB expression ($P < 0.0001$).

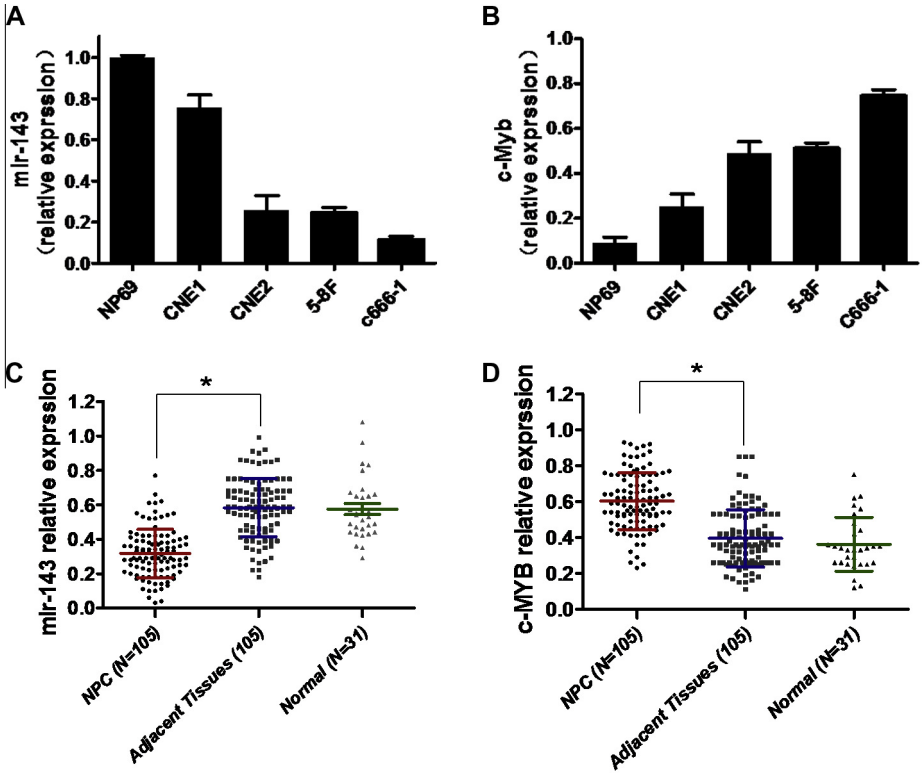

Fig. 1. MiR-143 was down-regulated and c-MYB was up-regulated in nasopharyngeal carcinoma (NPC) cells and clinical specimens. Expression of miR-143 (A) and c-MYB (B) in NPC cells. Bars represent mean values ± S.D. of three independent experiments; $^{*}P < 0.05$, $^{**}P < 0.05$. The relative expression levels of miR-143 (C) and c-MYB (D) in NPC tissues and matched normal tissues as detected by q-RT-PCR ($^{*}P < 0.05$).

Table 1
Correlation between c-Myb expression levels of tumors and clinical variables.

Variables	*n*	c-Myb (*n*, %)			miR-143 (*n*, %)		
		Low	High	*P*	Low	High	*P*
Gender							
Male	56	24 (42.9)	32 (57.1)		30 (53.6)	26 (46.4)	
Female	49	23 (46.9)	26 (53.1)	0.675	26 (53.1)	23 (46.9)	0.958
Age (years)							
>38	75	34(45.3)	41(54.7)		39(52.0)	36(48.0)	
⩽38	30	13(43.3)	17(56.7)	0.852	17(56.7)	13(43.3)	0.665
Histological subtype							
DNKC	83	40 (48.2)	43 (51.8)		41 (49.4)	42 (50.6)	
UDC	22	7 (31.8)	15 (68.2)	0.170	15 (68.2)	7 (31.8)	0.116
T classification							
T1–T2	50	28 (56.0)	22 (44.0)		20 (40.0)	30 (60.0)	
T3–T4	55	19 (34.5)	36 (65.5)	0.027*	36 (65.5)	19 (34.5)	0.009*
N classification							
N0–N1	63	34 (54.0)	29 (46.0)		40 (63.5)	23 (36.5)	
N2–N3	42	13 (31.0)	29 (69.0)	0.020*	16 (38.1)	26 (61.9)	0.011*
Distant metastasis							
No	56	36 (64.3)	20 (35.7)		23 (41.1)	33 (58.9)	
Yes	49	11 (22.4)	38 (77.6)	0.000*	33 (67.3)	16 (32.7)	0.007*
Clinical stage							
I–II	53	40 (75.5)	13 (24.5)		15 (28.3)	38 (71.1)	
III–IV	52	7 (44.8)	45 (55.2)	0.000*	41 (78.8)	11 (21.2)	0.000*

DNKC, differentiated non-keratinizing carcinoma; UDC, undifferentiatied carcinoma; T, tumor size; N, lymph node ($^{*}P < 0.05$).

3.3. Down-regulated expression of c-MYB inhibits cell growth in NPC cells

The results described above clearly demonstrated that c-MYB is highly expressed in NPC tissues and cells. In order to further clarify the role of c-MYB in NPC cells, we used c-MYB inhibitors (c-MYBi) to inhibit the expression of c-MYB in 5-8F and CNE2 cells. The inhibitory effect of c-MYBi was detected using Western blot analysis (Fig. 3A). Because the effects of c-MYB1-#2 inhibitor were most obvious, we used this inhibitor in subsequent experiments.

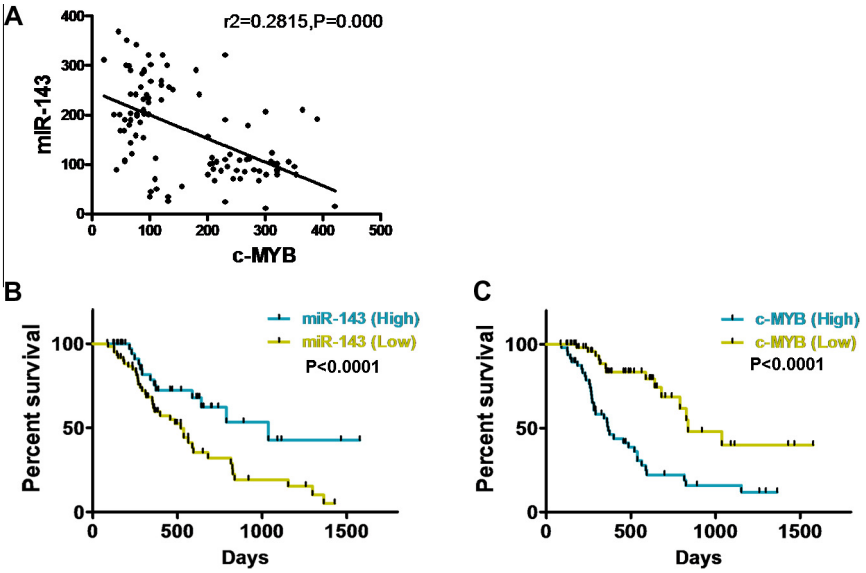

Fig. 2. Kaplan–Meier analysis of survival rate of patients with respect to c-MYB and miR-143 expression. (A) Correlation analysis of expression levels of c-MYB and miR-143 with patient survival. (B, C) The influence of c-MYB (B) and miR-143 (C) expression on the prognosis of patients with nasopharyngeal carcinoma.

To explore the effect of c-MYB on cell growth, 5-8F and CNE2 cells were transfected with either normal control (NC) or c-MYBi-#2. Results of a 3-(4,5-dimethylthiazol-2-yl)-2,5-diphenyltetrazolium bromide (MTT) assay showed that down-regulated c-MYB expression in cMYBi-#2-treated cells inhibited the growth of 5-8F cells by 2-fold ($P < 0.05$) and that CNE2 cells by 2.1-fold ($P < 0.05$) compared to control cells (Fig. 3B). Following the observation of c-MYBi-mediated growth inhibition, we examined its effect on colony formation rate and the cell-cycle distribution (Fig. 3C and D). The colony formation rate was significantly decreased in c-MYBi-treated cells when compared with NC MYB-expressing cells ($P < 0.05$). Furthermore, the proportion of cells at the G2/M phase was significantly reduced in the 5-8F and CNE2 cells after transfection with c-MYBi ($P < 0.05$). Next, we examined the expression of cell cycle-related proteins. Previous research has indicated that cyclin B1 is the main regulatory element of the cell cycle's G2 restriction point [14]. In addition, it is known that cyclin D1 is the main regulatory element of the G1/S phase [15]. As shown in Fig. 3E, after inhibition of c-MYB expression by c-MYBi, cyclin B1 protein expression was down-regulated, whereas cyclin D1 protein expression was up-regulated.

3.4. c-MYB directly regulates miR-143 expression

Sequence analysis of the miR-143 promoter revealed potential c-MYB binding sites (MBSs) within 2.0 kb of the transcriptional start site. These sites were designated as 1881 MBS-A, 1717 MBS-B, and 628 MBS-C, based on their respective upstream positions with reference to the transcriptional start site (Fig. 4A). To determine whether endogenous c-MYB could physically associate with these conserved MBSs within the miR-143 promoter, we used a chromatin immunoprecipitation (ChIP) analysis in CNE2 cells for all the putative MBSs. As shown in Fig. 4B, ChIPs were carried out with anti-c-MYB antibody and precipitated significant amounts of DNA product when compared with the control reactions used. The control experiments included in these ChIP assays were performed under identical conditions except for the use of anti-IgG instead of the c-MYB antibodies. The ChIP results revealed that c-MYB was most significantly bound to MBS-C within the miR-143 promoter. Knockdown of c-MYB diminished the amount of MBS-C DNA that could be immunoprecipitated by the c-MYB antibody (Fig. 4D). This suggested that c-MYB is directly and specifically associated with this promoter region.

To examine the potential physiological significance of c-MYB protein binding to the miR-143 promoter, miR-143 expression levels were examined in CNE2 cells after being treated with small hairpin (shRNA) targeted to the endogenous c-MYB mRNA. Results of q-RT-PCR showed that c-MYB mRNA expression was reduced 48 hours after CNE2 cells were transfected with the c-MYB-targeted shRNA. Delivery of these shRNAs into CNE2 cells also resulted in an increase in miR-143 levels (Fig. 4C and E).

3.5. c-MYB promotes the NPC CSCs through down-regulation of miR-143

To elucidate whether c-MYB regulation of miR-143 could also influence CSC properties, we down-regulated c-MYB expression using c-MYBi and co-expressed miR-143 mimics in 5-8F and CNE2 cells. NC-transfected cells were used as control groups. As shown in Fig. 5A, Western blot analysis was carried out for vimentin, E-cadherin, SOX-2, and NANOG. This allowed us to evaluate specific CSC characteristics of the 5-8F and CNE2 cell lines. The results indicated that the epithelial markers of E-cadherin and vimentin were increased and decreased, respectively. The stem cell surface markers SOX-2 and NANOG were decreased in 5-8F and CNE2 cells. To examine whether CSCs were affected after c-MYBi and miR-143 treatment, we detected CSCs using Aldefluor analyses and CD44 immuno label (Fig. 5B; Supplementary Fig. 1). When compared with the control, c-MYBi reduced by 1.1% and 1.3% in ALDH-positive population, and 2.9% and 3.3% in CD44-positive population, while cells co-expressing c-MYBi and miR-143 showed a reduction in the ALDH-positive population by 0.3% and 0.6%, and CD44-positive population by 0.6% and 0.3% for 5-8F and CNE2 cells, respectively. We next inhibited c-MYB in the 5-8F and CNE2 cells over-expressing miR-143 and found that the number and size of tumorspheres formed were significantly reduced compared to those in cells treated with only c-MYBi (Fig. 5C). In order to determine the impact of c-MYB-regulated miR-143 expression on stem cell makers, an immunofluorescence analysis was performed, which revealed that SOX-2 was strongly and equally expressed in the nuclei of 5-8F and CNE2 cells. SOX-2 was expressed at low levels in the nuclei of co-transfected cells (Fig. 5D). The expression

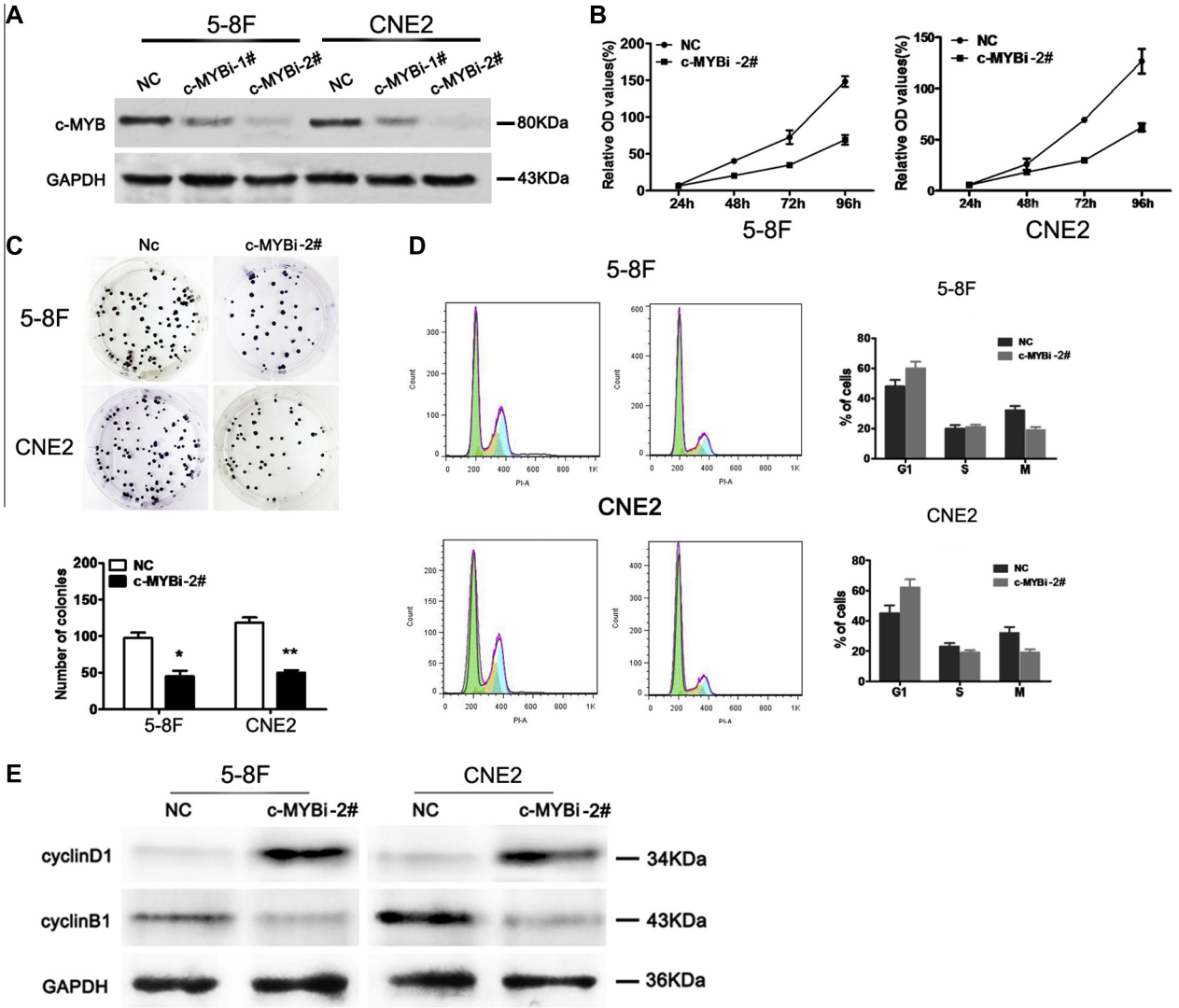

Fig. 3. Low expression of c-MYB inhibits cell growth in cancer cells. (A) Western blot analysis of c-MYB expression in 5-8F and CNE2 cells. GAPDH was used as the loading control. (B) Statistical plots of three independent cell growth assays. 5-8F and CNE2 cells were transfected and harvested at different times, as indicated. (C) Representative images of the colony formation assay of c-MYBi-infected 5-8F and CNE2 cells. Colonies were evaluated and values are reported as the ratio between c-MYB-targeted shRNA-infected cells and vector-infected cells. Bars represent the mean ± S.D. of three independent experiments; $^{*}P < 0.05$, $^{**}P < 0.05$. (D) Representative histograms for cell-cycle distributions of 5-8F and CNE2 cells transfected with c-MYBi. (E) Western blot analysis of cyclin B1 and cyclin D1 expression in 5-8F and CNE2 cells. GAPDH was used as the loading control.

of c-MYB, NANOG, and SOX-2 protein was measured in 27 NPC samples using immunohistochemical staining. The results showed that c-MYB was highly expressed in the nucleus. NANOG and SOX-2 were observed both in the cytoplasm and nucleus of cancer cells (Fig. 5E).

3.6. Induction of radiation resistance in NPC cells by c-MYB regulation of the miR-143 promoter

Many studies have reported the importance of CSC-induced transdifferentiation on radiosensitivity. We observed that c-MYB negatively regulated the expression of miR-143, which reduced the enrichment of CSCs. In order to elucidate the relationship between c-MYB and radiosensitivity, we compared the radiation response of NPC cells with different levels of c-MYB. When 5-8F and CNE2 cells were seeded at increasing densities and exposed to ionizing radiation, cells with down-regulated expression of c-MYB were found to be significantly less resistant to radiation than vector-transfected cells (Fig. 6A). We also found up-regulation of cleaved caspase-3 and cleaved PARP following 8-Gy irradiation treatment via Western blotting in NPC cell lines in the control group. Conversely, in cells with down-regulated expression of c-MYB, the expression of cleaved caspase-3 and cleaved PARP did not increase. This indicated that c-MYB might have induced reduced apoptosis by preventing caspase-3 and PARP cleavage (Fig. 6B).

To confirm that radiation treatment induces apoptosis, we transfected c-MYBi, miR-143, or vector control into the 5-8F and CNE2 cells, and the cells were double-stained with Annexin V/7-AAD and subjected to flow cytometry analysis. The results revealed that the percentage of apoptotic 5-8F and CNE2 cells increased from 6.85% to 11.66% and from 7.00% to 11.79% in 5-8F and CNE2 cells, respectively, following 8-Gy irradiation for 24 h (Fig. 6C).

To determine whether c-MYB and miR-143 affected double-strand break (DSB) repair, we measured the extent of unrepaired DNA damage. This was performed using a single-cell neutral comet assay in 5-8F and CNE2 cells transfected with c-MYBi or

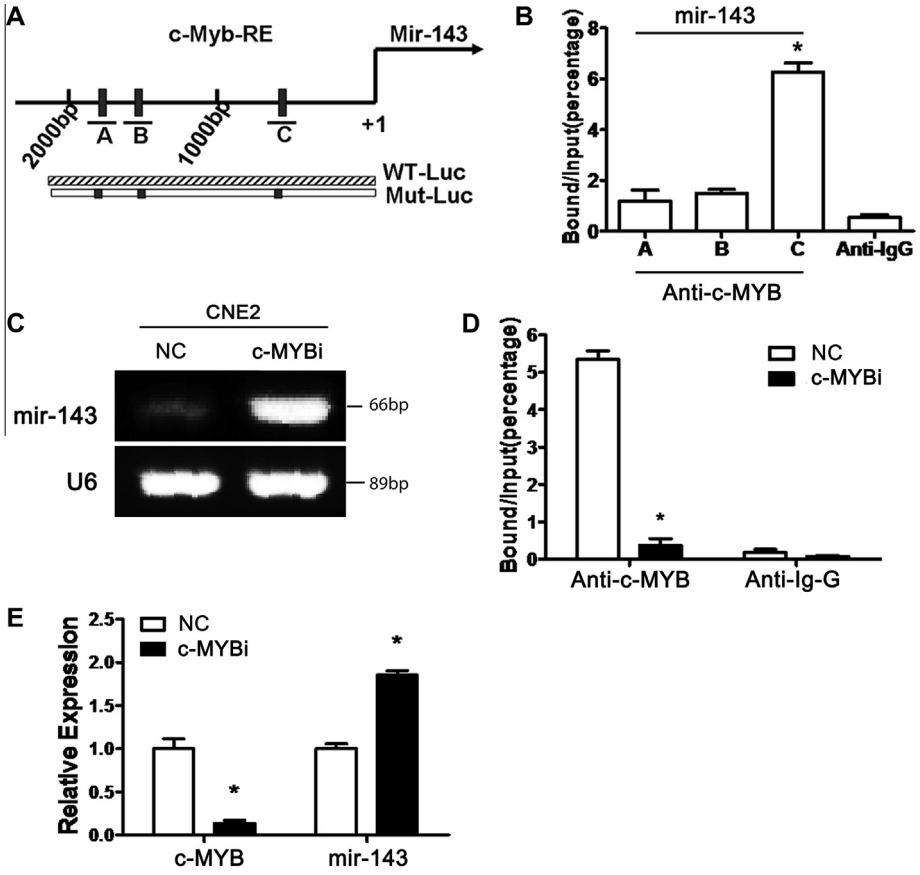

Fig. 4. c-MYB directly regulates miR-143 expression. (A) Diagram of the c-MYB-binding sites within 2000 bp of the transcriptional start site for miR-143. (B) ChIP assay using antibodies against c-MYB on CNE2 cells. Levels of c-MYB-binding sites (A–C) immunoprecipitated by anti-c-MYB are shown. Results represent three independent experiments, mean + S.D.; $^{*}P < 0.05$. (C) Expression levels of miR-143 after CNE2 cells were transfected with c-MYB shRNA for 48 h. (D) ChIP assay using antibodies against c-MYB on CNE2 cells with silenced c-MYB expression. Levels of c-MYB-binding site C bound by c-MYB. The results are the mean values + S.D. of three independent experiments, $^{*}P < 0.05$. (E) c-MYB shRNA up-regulated miR-143 expression in CNE2 cells. The results are the mean values + S.D. of three independent determinations, $^{*}P < 0.05$.

co- transfected with c-MYBi and miR-143. The comet tail moment quantifies the extent of unrepaired DNA damage. After 8-Gy radiation exposure, the frequency of comet tails was higher ($P < 0.05$) in 5-8F and CNE2 cells co-expressing c-MYBi and miR-143 as compared to those only expressing c-MYBi ($P < 0.05$, Fig. 6D).

4. Discussion

NPC therapy often fails because patients develop high resistance to chemotherapy and radiotherapy. Therapeutic resistance is likely due to multiple factors. Some studies found that a highly tumorigenic subpopulation of stem cell-like NPC cells are highly resistant to radiation and chemotherapies. Understanding the molecular mechanisms underlying this NPC phenotype will be crucial for developing a therapeutic approach to overcome NPC radioresistance. In this study, the expression levels of c-MYB and miR-143 were found to be up- and down-regulated, respectively, in NPC compared to normal tissue. Furthermore, down-regulated expression of c-MYB significantly inhibited NPC cell proliferation. We also found that c-MYB directly regulated the expression of miR-143. Interestingly, miR-143 regulation by c-MYB was critical for the CSC phenotype and radiosensitivity of NPCs.

c-MYB has been associated with cell proliferation and differentiation regulation in leukemia and colon cancer. The proliferation of malignant cells is often accompanied by high levels of c-MYB expression, whereas benign differentiation of tumor cells requires down-regulation of c-MYB [2,16]. Furthermore, we examined the different degrees of malignancy in human NPC specimens. c-MYB and the stem cell surface markers SOX-2 and NANOG were widely expressed at all levels of NPC malignancy. This phenomenon was also verified in NPC cell lines. We compared the levels of c-MYB expression in NPC patient samples and found a significant association with distant metastasis. Furthermore, c-MYB expression was significantly higher in patients at clinical stage III–IV compared to those at stage I–II ($P < 0.05$). Similarly, a previous study showed that 82% of adenoid cystic carcinomas of the head and neck stained positive for MYB protein as compared with non-adenoid cystic carcinoma neoplasms. This was an indication that MYB immunostaining might be useful for the diagnosis of adenoid cystic carcinoma [17]. Kim et al. examined c-MYB expression in malignant tissue specimens from 10 patients with head and neck squamous cell carcinoma (HNSCC) [18]. Over-expression of shRNA targeting MYB in HNSCC cells inhibited in vitro cell proliferation. Furthermore, the expression of growth factors such as insulin-like growth factor (IGF)-I, -II, -1R, and vascular endothelial growth factor (VEGF) inhibited Akt/PKB pathway activation and enhanced induction of apoptosis. Previous studies have shown that the c-MYB protein induced specific effects on the cell cycle at G1/S and on regulation of T cell proliferation. In particular, c-MYB expression is relatively high in cells that are in the late G1 phase entering the S phase [19]. In this study, we found that over-expression of c-MYB significantly stimulated the growth of NPC cells through a shortened G1 phase and an extended S/G2 phase. These results suggest that c-MYB might play a role in the cellular growth, development, and proliferation of NPC. MiR-143 is known to be down-regulated in NPC. Furthermore, studies have shown that miR-143 is down-regulated in

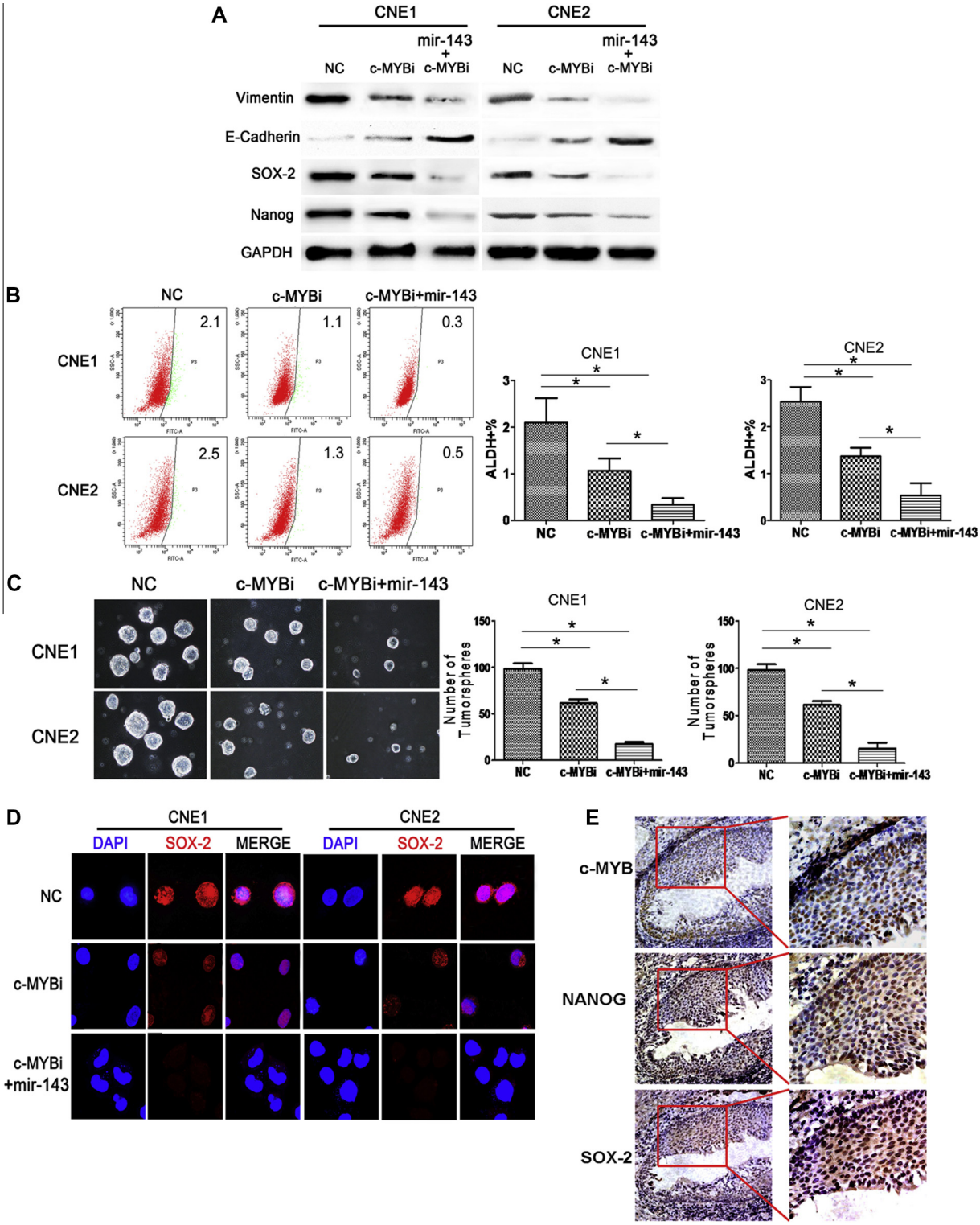

Fig. 5. c-MYB promotes NPC cancer stem cell markers through upregulation of miR-143. (A) Western blot analysis of vimentin, E-cadherin, SOX-2, and NANOG expression in 5-8F and CNE2 cells. GAPDH was used as the loading control. (B) Left panel: Aldefluor assay of the proportion of ALDH+ cells among total number of 5-8F and CNE2 cells. Right panel: Percentage of ALDH+ cells. Results were expressed as the mean ± S.D. of three separate trials; $^{*}P < 0.05$. (C) Left panel: Representative images of irradiated (8 Gy) 5-8F and CNE2 cells that were seeded in tumorsphere culture medium at 1000 cells/well for 7 days. Right panel: Data shown represent the average sphere count from a representative experiment performed in triplicate wells. Data represent the mean value ± S.D.; $n = 3$, $*P < 0.05$. (D) Immunofluorescence detection of SOX-2 expression in 5-8F and CNE2 cells. (E) Immunohistochemical staining of c-MYB, NANOG, and SOX-2 in nasopharyngeal carcinoma tissues (magnification 400× for all images).

front-specific tumor invasion, which is associated with an aggressive mucinous phenotype in colorectal cancer [21,22]. In a mouse colorectal carcinoma xenograft study, overexpression of miR-143 impaired tumor growth by induction of apoptosis and inhibition of proliferation [23]. Other miRNAs are also considered to have tumor suppressor activity and are also down-regulated in cancers,

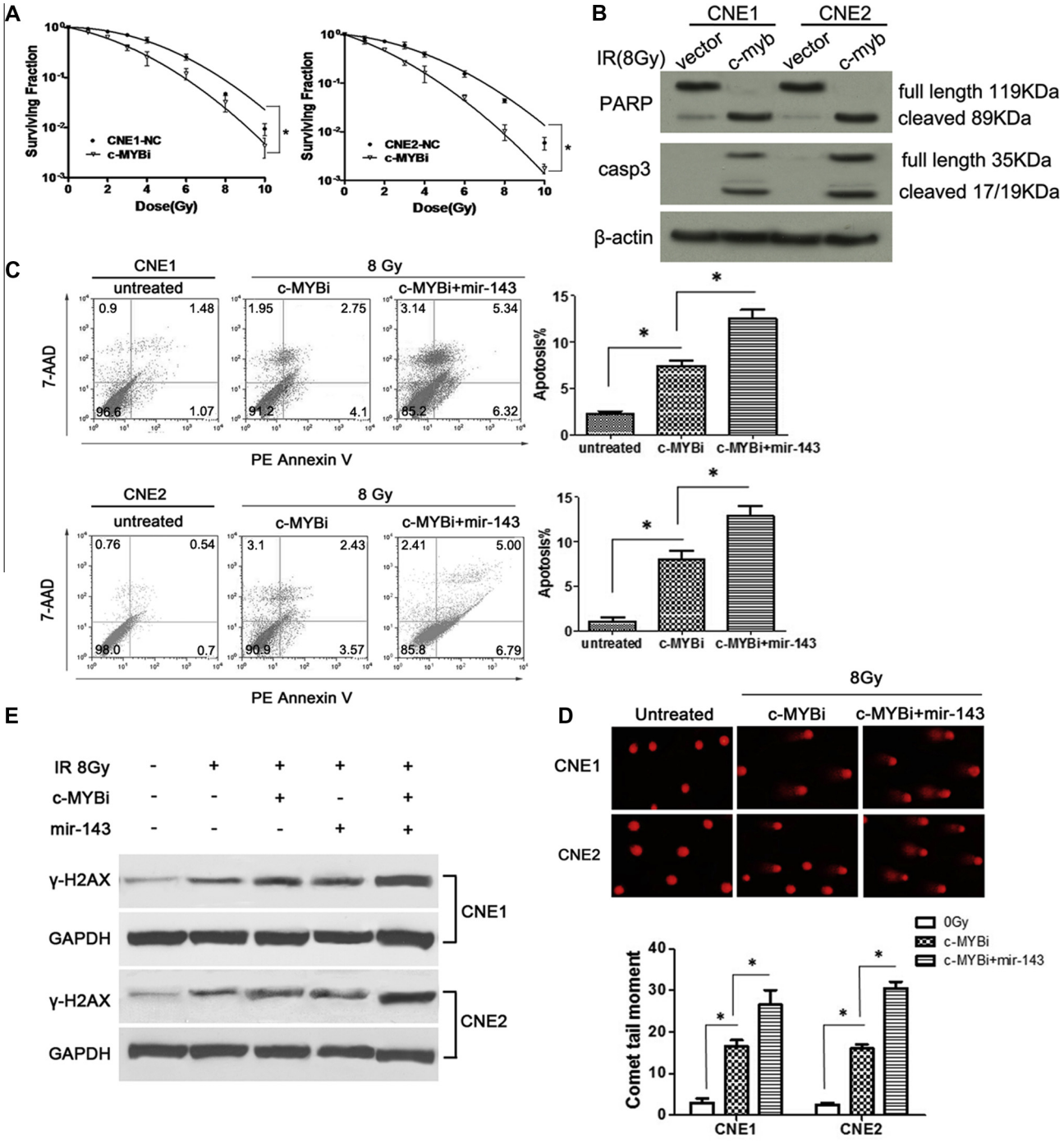

Fig. 6. c-MYB regulation of the miR-143 promoter in nasopharyngeal carcinoma cells results in radiation resistance. (A) Clonogenic survival of 5-8F and CNE2 cells seeded at different densities. (B) Representative Western blot analysis of caspase 3, PARP, cleaved caspase 3, and cleaved PARP in 5-8F and CNE2 cells. GAPDH was used as the loading control. (C) Left panel: The Annexin V/7AAD double-staining method was used to detect the percentage of apoptosis after c-MYB over-expression and radiation exposure of c-MYB/miR-143-transfected 5-8F and CNE2 cells. Right panel: Percentage of apoptosis cells. Results were expressed as the mean ± S.D. of three separate trials; $^{*}P < 0.05$. (D) Representative images of the comet assay used to detect DNA double-strand breaks (DSBs) in 5-8F and CNE2 cells due to radiation. Histogram of the comet assay data. The results are the mean value ± S.D. of three independent experiments; $^{*}P < 0.05$, $^{**}P < 0.05$. Induction of DSBs by c-MYB and/or miR-143 in the radiation-exposed 5-8F and CNE2 cells was assessed using a neutral comet assay. (E) Representative Western blot analysis of γ-H2AX in 5-8F and CNE2 cells. GAPDH was used as the loading control.

including let-7, miR-15, miR-16, miR-17-5p, miR-29, miR-34, miR-124a, miR-127, miR-145, and miR-181 [24]. To validate the direct association between c-MYB and miR-143 promoters, we performed ChIP analyses in CNE2 cells using an antibody specific to c-MYB. The ChIP results revealed that c-MYB most significantly bound to MBS-C within the miR-143 promoter. Next, we showed that down-regulation of c-MYB expression in CNE2 cells effectively promoted miR-143 expression at the mRNA level. This suggested a potential inverse relationship between miR-143 and c-MYB in NPC. Clinically, the main reason for treatment failure is disease recurrence and metastasis. Recent research has focused on recurrence in CSCs, a small subpopulation of tumor cells that are tumor-initiating and drive the production of cancer cells. Progress in this field has highlighted the necessity of targeting these cells as

they strongly determine the response to treatment [25]. An important relationship between c-MYB and CSCs was recently reported, with important implications for breast cancer cell invasion and metastasis [26]. In this study, the down-regulation of c-MYB in human NPC cells (5-8F and CNE2) reduced CSC enrichment and caused a loss of epithelial and gain of mesenchymal markers, indicating its role in EMT [27]. c-MYB is also involved in liver CSC self-renewal, potentially via modulation of miR-150 that interacts with the 3′ untranslated region of c-MYB mRNA, as overexpression of miR-150 down-regulates c-MYB protein levels [28]. Peng et al. examined bone metastasis of prostate cancer and found that down-regulation of miR-143 and -145 was negatively correlated with bone metastasis [29]. We used c-MYB shRNA to transfect 5-8F and CNE2 cells, which resulted in increased expression of miR-143. As a result the significantly inhibited ALDH+ cell population, 5-8F and CNE2 cells showed a reduced number of tumorspheres. These findings indicate that miR-143 and c-MYB expression could be associated with metastasis of NPC, and suggest that they might also play an important role in the metastasis and regulation of CSCs. Radiation therapy plays an important role in NPC treatment. However, recurrence is observed in most patients, and some patients even develop radioresistance that might limit any further treatment. It is well known that CSCs play an important role in tumor progression and recurrence [25,30]. Furthermore, CSCs are reported to be related to the development of radioresistance in many cancers [31]. Studies have demonstrated that delivering high doses of radiation to breast cancer cells induces the cells to exhibit the classic hallmarks of CSCs, which ultimately promote increased cancer cell recurrence [32]. Our study of gradient-dose irradiation showed high c-MYB expression in cells with enhanced radiation resistance. Ionizing radiation leads to cell death through the production of unrepairable DNA DSBs. A hallmark of DNA DSB recognition and repair is histone H2A phosphorylation, which is thought to mark specific sites of DNA damage [33]. By detecting DNA damage in individual cells (via analysis of histone H2AX phosphorylation), we found that c-MYBi and miR-143 co-expression in 5-8F and CNE2 cells could lead to DNA damage repair and recovery of radiation sensitivity. In summary, our findings suggest that c-MYB might play an important role in the metastasis of NPC. By further focusing on the role of miR-143 in regulating NPC stem cells, regulation of radiation resistance of NPC cells might be achieved. Understanding the molecular mechanisms that potentiate radioresistance is critical for the development of new radiotherapeutic strategies to overcome this carcinoma.

Funding

This work was supported by a grant from the National Natural Science Funds of China (No. 81301939).

Conflicts of interest statement

The authors do not have any potential conflicts of interest.

Acknowledgements

We thank Professor Gao from The First Affiliated Hospital of Zhengzhou University for providing the human nasopharyngeal carcinoma specimens.

Appendix A. Supplementary data

Supplementary data associated with this article can be found, in the online version, at http://dx.doi.org/10.1016/j.febslet.2015.01.012.

References

[1] Kim, K.H., Seol, H.J., Kim, E.H., Rheey, J., Jin, H.J., Lee, Y., Joo, K.M., Lee, J. and Nam, D.H. (2012) Wnt/beta-catenin signaling is a key downstream mediator of MET signaling in glioblastoma stem cells. Neuro. Oncol.
[2] Ramsay, R.G. and Gonda, T.J. (2008) MYB function in normal and cancer cells. Nat. Rev. Cancer 8, 523–534.
[3] Ramsay, R.G., Barton, A.L. and Gonda, T.J. (2003) Targeting c-Myb expression in human disease. Expert Opin. Ther. Targets 7, 235–248.
[4] Cheasley, D., Pereira, L., Lightowler, S., Vincan, E., Malaterre, J. and Ramsay, R.G. (2011) Myb controls intestinal stem cell genes and self-renewal. Stem Cells 29, 2042–2050.
[5] Bartel, D.P. (2004) MicroRNAs: genomics, biogenesis, mechanism, and function. Cell 116, 281–297.
[6] Ambros, V. (2004) The functions of animal microRNAs. Nature 431, 350–355.
[7] Kloosterman, W.P. and Plasterk, R.H. (2006) The diverse functions of microRNAs in animal development and disease. Dev. Cell 11, 441–450.
[8] Nelson, P., Kiriakidou, M., Sharma, A., Maniataki, E. and Mourelatos, Z. (2003) The microRNA world: small is mighty. Trends Biochem. Sci. 28, 534–540.
[9] Chistiakov, D.A. and Chekhonin, V.P. (2012) Contribution of microRNAs to radio- and chemoresistance of brain tumors and their therapeutic potential. Eur. J. Pharmacol. 684, 8–18.
[10] Akao, Y., Nakagawa, Y. and Naoe, T. (2006) MicroRNAs 143 and 145 are possible common onco-microRNAs in human cancers. Oncol. Rep. 16, 845–850.
[11] Takagi, T., Iio, A., Nakagawa, Y., Naoe, T., Tanigawa, N. and Akao, Y. (2009) Decreased expression of microRNA-143 and -145 in human gastric cancers. Oncology 77, 12–21.
[12] Noguchi, S., Mori, T., Hoshino, Y., Maruo, K., Yamada, N., Kitade, Y., Naoe, T. and Akao, Y. (2011) MicroRNA-143 functions as a tumor suppressor in human bladder cancer T24 cells. Cancer Lett. 307, 211–220.
[13] Lin, T., Dong, W., Huang, J., Pan, Q., Fan, X., Zhang, C. and Huang, L. (2009) MicroRNA-143 as a tumor suppressor for bladder cancer. J. Urol. 181, 1372–1380.
[14] Kawamoto, H., Koizumi, H. and Uchikoshi, T. (1997) Expression of the G2-M checkpoint regulators cyclin B1 and cdc2 in nonmalignant and malignant human breast lesions: immunocytochemical and quantitative image analyses. Am. J. Pathol. 150, 15–23.
[15] Shimonishi, S., Muraguchi, T., Mitake, M., Sakane, C., Okamoto, K. and Shidoji, Y. (2012) Rapid downregulation of cyclin D1 induced by geranylgeranoic acid in humanhepatoma cells. Nutr. Cancer.
[16] Stenman, G., Andersson, M.K. and Andren, Y. (2010) New tricks from an old oncogene: gene fusion and copy number alterations of MYB in human cancer. Cell Cycle 9, 2986–2995.
[17] Brill 2nd, L.B., Kanner, W.A., Fehr, A., Andren, Y., Moskaluk, C.A., Loning, T., Stenman, G. and Frierson Jr, H.F. (2011) Analysis of MYB expression and MYB-NFIB gene fusions in adenoid cystic carcinoma and other salivary neoplasms. Mod. Pathol. 24, 1169–1176.
[18] Kim, S.Y., Yang, Y.S., Hong, K.H., Jang, K.Y., Chung, M.J., Lee, D.Y., Lee, J.C., Yi, H.K., Nam, S.Y. and Hwang, P.H. (2008) Adenovirus-mediated expression of dominant negative c-myb induces apoptosis in head and neck cancer cells and inhibits tumor growth in animal model. Oral Oncol. 44, 383–392.
[19] Quintana, A.M., Zhou, Y.E., Pena, J.J., O'Rourke, J.P. and Ness, S.A. (2011) Dramatic repositioning of c-Myb to different promoters during the cell cycle observed by combining cell sorting with chromatin immunoprecipitation. PLoS ONE 6, e17362.
[20] Lun, S.W., Cheung, S.T., Cheung, P.F., To, K.F., Woo, J.K., Choy, K.W., Chow, C., Cheung, C.C., Chung, G.T., Cheng, A.S., Ko, C.W., Tsao, S.W., Busson, P., Ng, M.H. and Lo, K.W. (2012) CD44+ cancer stem-like cells in EBV-associated nasopharyngeal carcinoma. PLoS ONE 7, e52426.
[21] Chang, K.H., Miller, N., Kheirelseid, E.A., Lemetre, C., Ball, G.R., Smith, M.J., Regan, M., McAnena, O.J. and Kerin, M.J. (2011) MicroRNA signature analysis in colorectal cancer: identification of expression profiles in stage II tumors associated with aggressive disease. Int. J. Colorectal Dis. 26, 1415–1422.
[22] Kahlert, C., Klupp, F., Brand, K., Lasitschka, F., Diederichs, S., Kirchberg, J., Rahbari, N., Dutta, S., Bork, U., Fritzmann, J., et al. (2011) Invasion front-specific expression and prognostic significance of microRNA in colorectal liver metastases. Cancer Sci. 102, 1799–1807.
[23] Borralho, P.M., Simoes, A.E., Gomes, S.E., Lima, R.T., Carvalho, T., Ferreira, D.M., Vasconcelos, M.H., Castro, R.E. and Rodrigues, C.M. (2011) MiR-143 overexpression impairs growth of human colon carcinoma xenografts in mice with induction of apoptosis and inhibition of proliferation. PLoS ONE 6, e23787.
[24] Croce, C.M. (2009) Causes and consequences of microRNA dysregulation in cancer. Nat. Rev. Genet. 10, 704–714.
[25] Hepburn, A.C., Veeratterapillay, R., Williamson, S.C., El-Sherif, A., Sahay, N., Thomas, H.D., Mantilla, A., Pickard, R.S., Robson, C.N. and Heer, R. (2012) Side population in human non-muscle invasive bladder cancer enriches for cancer stem cells that are maintained by MAPK signalling. PLoS ONE 7, e50690.
[26] Knopfova, L., Benes, P., Pekarcikova, L., Hermanova, M., Masarik, M., Pernicova, Z., Soucek, K. and Smarda, J. (2012) C-Myb regulates matrix metalloproteinases 1/9, and cathepsin D: implications for matrix-dependent breast cancer cell invasion and metastasis. Mol. Cancer 11, 15.
[27] Srivastava, S.K., Bhardwaj, A., Singh, S., Arora, S., McClellan, S., Grizzle, W.E., Reed, E. and Singh, A.P. (2012) Myb overexpression overrides androgen

depletion-induced cell cycle arrest and apoptosis in prostate cancer cells, and confers aggressive malignant traits: potential role in castration resistance. Carcinogenesis.
[28] Zhang, J., Luo, N., Luo, Y., Peng, Z., Zhang, T. and Li, S. (2012) MicroRNA-150 inhibits human CD133-positive liver cancer stem cells through negative regulation of the transcription factor c-Myb. Int. J. Oncol. 40, 747–756.
[29] Peng, X., Guo, W., Liu, T., Wang, X., Tu, X., Xiong, D., Chen, S., Lai, Y., Du, H., Chen, G., et al. (2011) Identification of miRs-143 and -145 that is associated with bone metastasis of prostate cancer and involved in the regulation of EMT. PLoS ONE 6, e20341.
[30] Zomer, A., Inge, J.E.S., Ritsma, L., Beerling, E., Vrisekoop, N. and van Rheenen, J. (2012) Intravital imaging of cancer stem cell plasticity in mammary tumors. Stem Cells, http://dx.doi.org/10.1002/stem.1296.
[31] Banerjee, A., Qian, P., Wu, Z.S., Ren, X., Steiner, M., Bougen, N.M., Liu, S., Liu, D.X., Zhu, T. and Lobie, P.E. (2012) ARTEMIN stimulates radio- and chemo-resistance by promoting TWIST1-BCL-2 dependent cancer stem cell-like behaviour in mammary carcinoma cells. J. Biol. Chem.
[32] Zhang, X., Li, X., Zhang, N., Yang, Q. and Moran, M.S. (2011) Low doses ionizing radiation enhances the invasiveness of breast cancer cells by inducing epithelial–mesenchymal transition. Biochem. Biophys. Res. Commun. 412, 188–192.
[33] Olive, P.L. (2004) Detection of DNA damage in individual cells by analysis of histone H2AX phosphorylation. Methods Cell Biol. 75, 355–373.